SAND2013-6417C

Exceptional service in the national interest

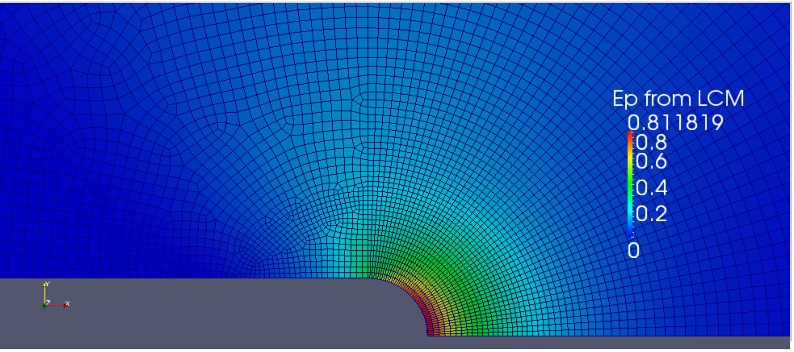

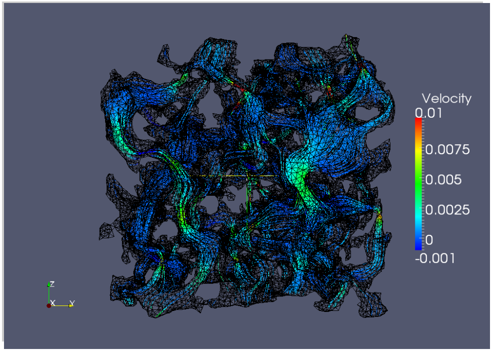

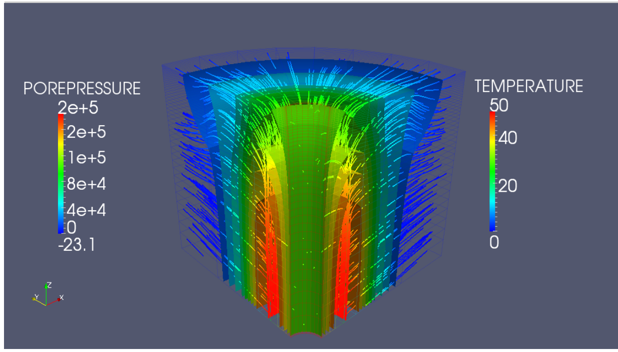

A stabilized finite element formulation for monolithic thermo-hydro-mechanical simulations at finite strain

WaiChing Sun, Jakob T Ostien, James W Foulk III
Mechanics of Materials Department
Sandia National Laboratories, California

Collaborators on Related Projects

- James W Foulk III, Sandia National Laboratories, CA
- Alejandro Mota, Sandia National Laboratories, CA
- Qiushi Chen, Sandia National Laboratories, CA (now Clemson University)
- Jonathan A Zimmerman, Sandia National Laboratories, CA
- Andrew Salinger, Sandia National Laboratories, NM

Motivations

Geothermal energy

Rainfall induced slope instability

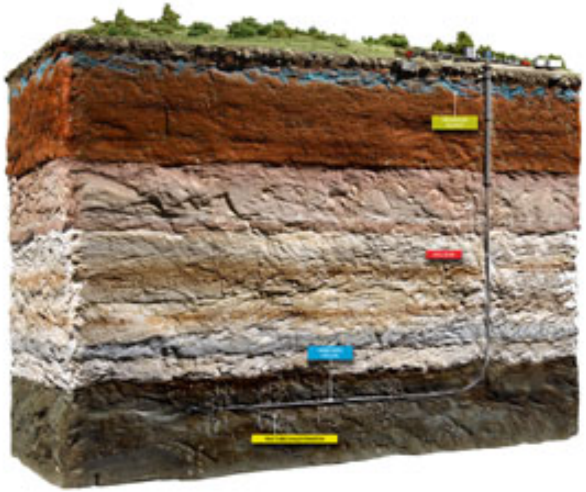

Hydraulic fracture (fracking)

Soil liquefaction

Multi-scale nature of porous media

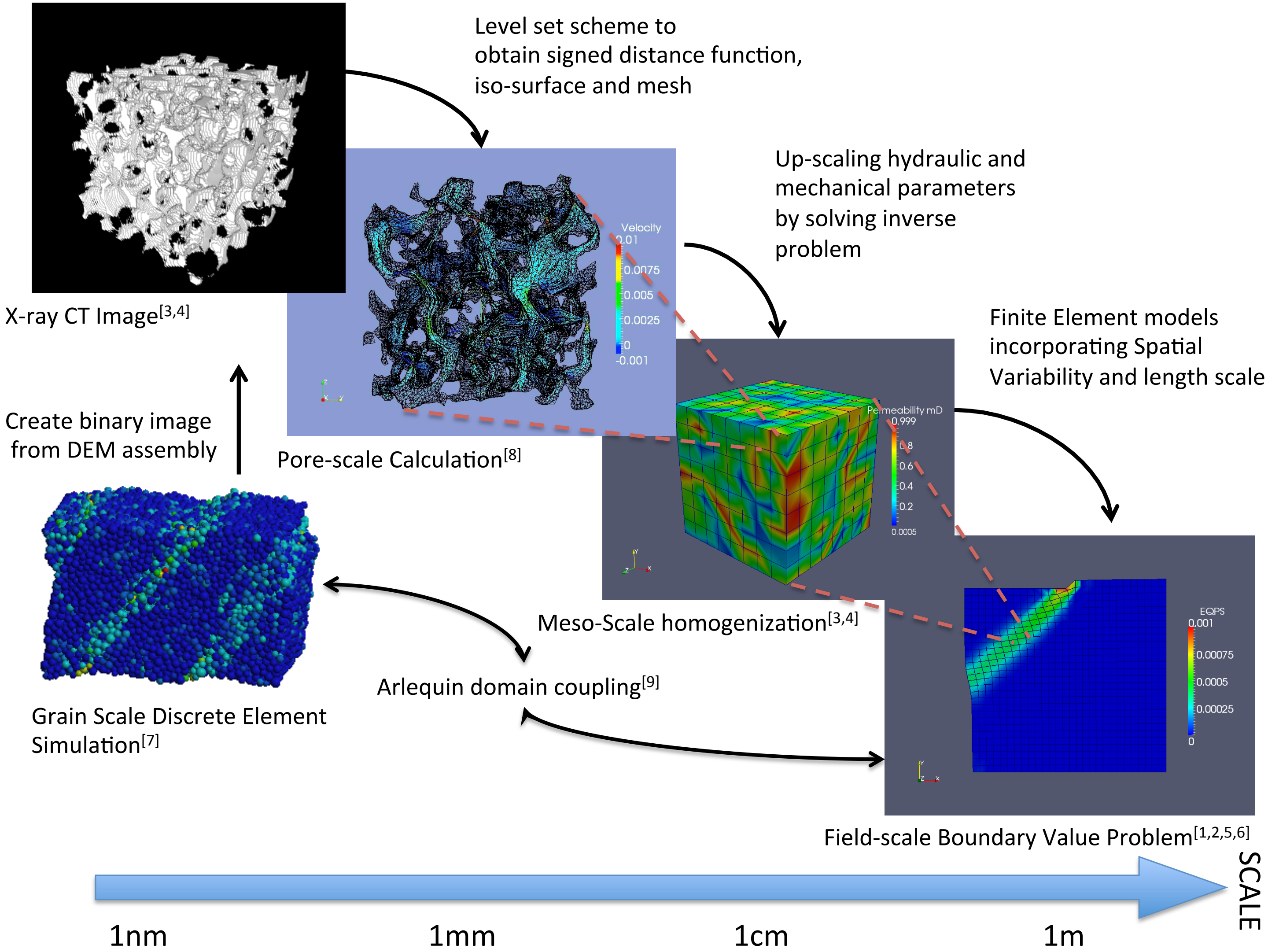

Level set scheme to
obtain signed distance function,
iso-surface and mesh

X-ray CT Image[3,4]

Pore-scale Calculation[8]

Up-scaling hydraulic and
mechanical parameters
by solving inverse
problem

Finite Element models
incorporating Spatial
Variability and length scale

Create binary image
from DEM assembly

Meso-Scale homogenization[3,4]

Arlequin domain coupling[9]

Grain Scale Discrete Element
Simulation[7]

Field-scale Boundary Value Problem[1,2,5,6]

SCALE

1nm 1mm 1cm 1m

Thermo-hydro-mechanics Finite Element Model at Continuum Scale

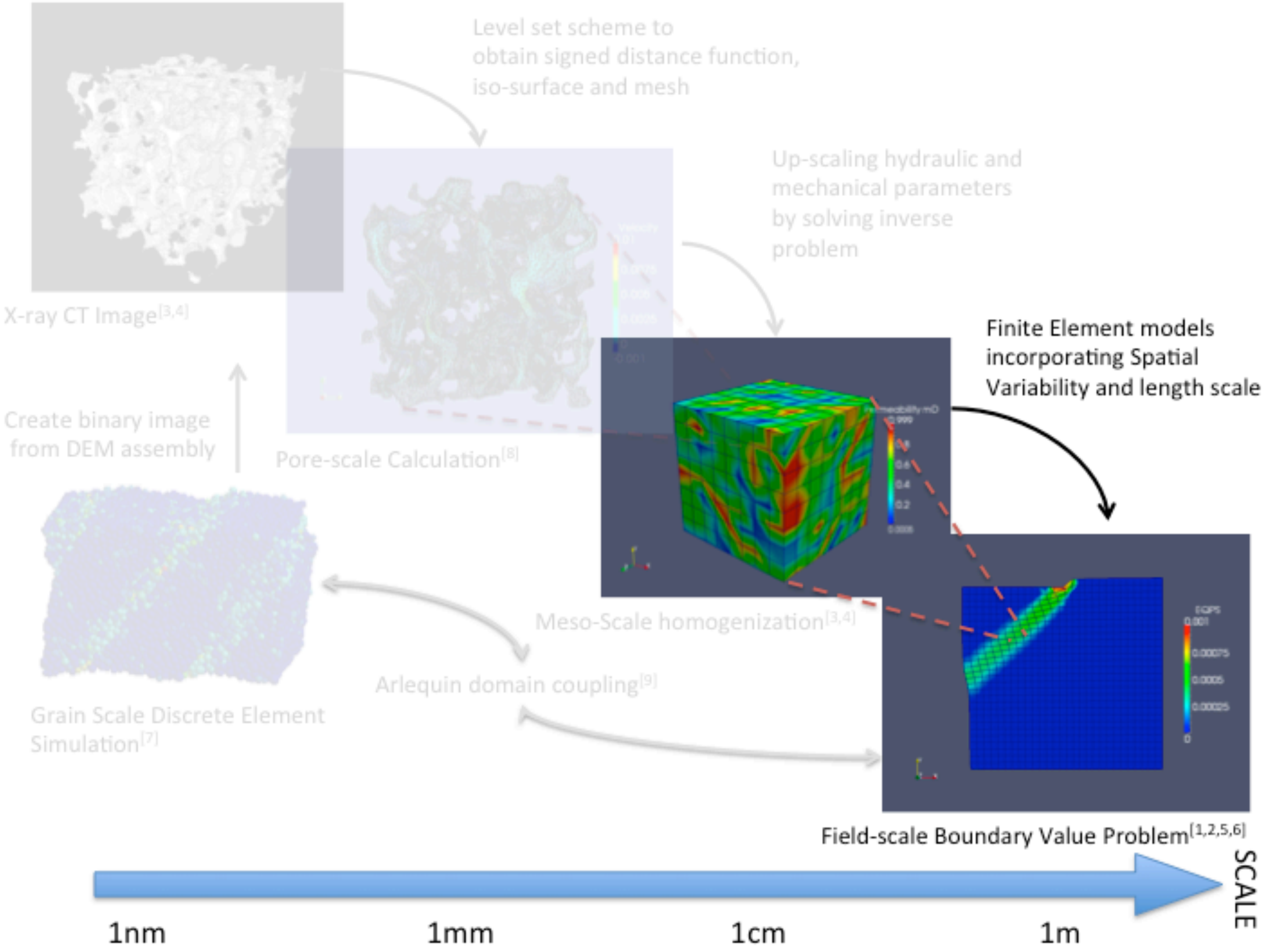

Level set scheme to obtain signed distance function, iso-surface and mesh

Up-scaling hydraulic and mechanical parameters by solving inverse problem

X-ray CT Image[3,4]

Finite Element models incorporating Spatial Variability and length scale

Create binary image from DEM assembly

Pore-scale Calculation[8]

Meso-Scale homogenization[3,4]

Arlequin domain coupling[9]

Grain Scale Discrete Element Simulation[7]

Field-scale Boundary Value Problem[1,2,5,6]

Key Features of THM Models

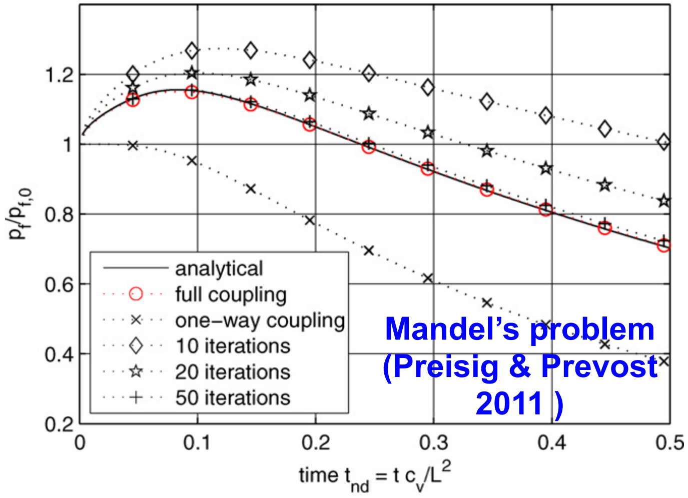

Mandel's problem (Preisig & Prevost 2011)

- ✓ Preserving Mandel-Cryer effect

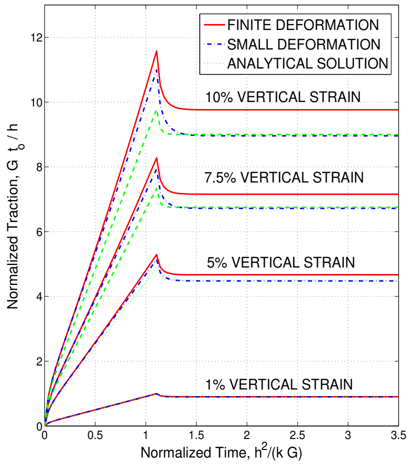

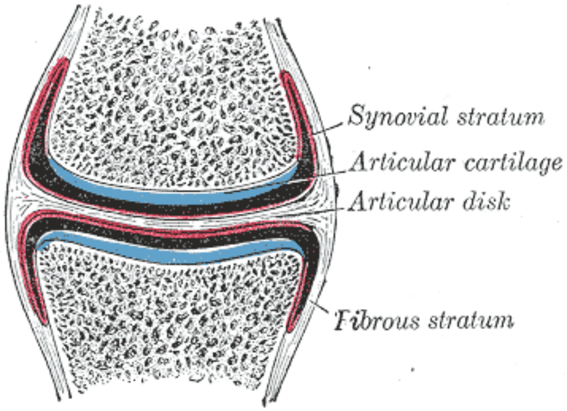

- ✓ Modeling large isochoric deformation at undrained limit or critical state without locking

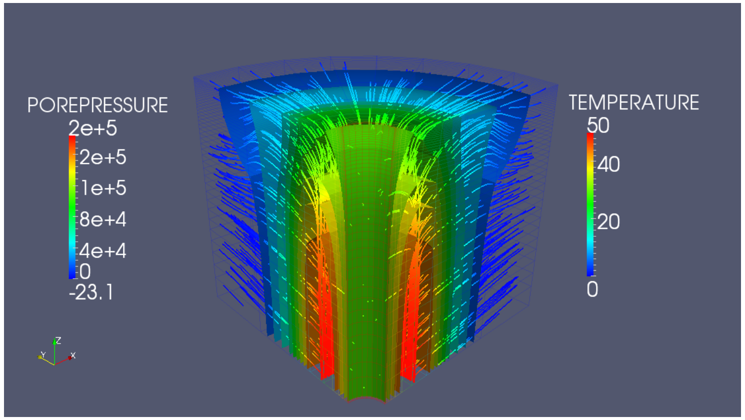

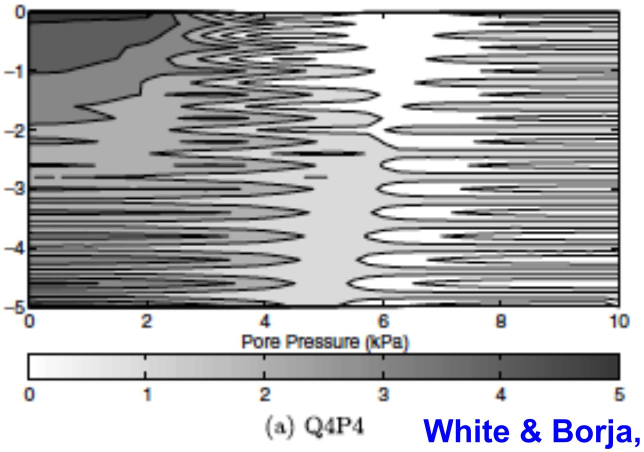

White & Borja, 2009

- ✓ Fully coupled thermo-hydro-mechanical coupling
- ✓ Eliminating spurious pressure mode due to lack of inf-sup condition

Kinematics of THM Problem at Finite Strain

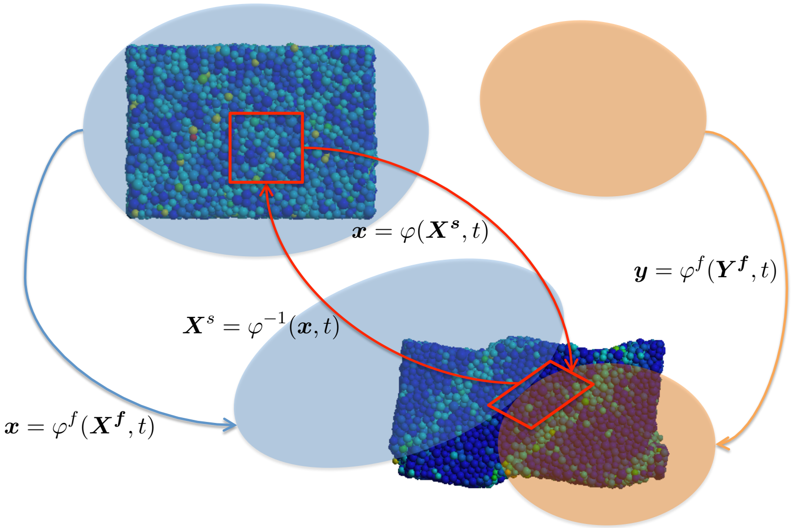

Trajectories of the solid and fluid constituent.

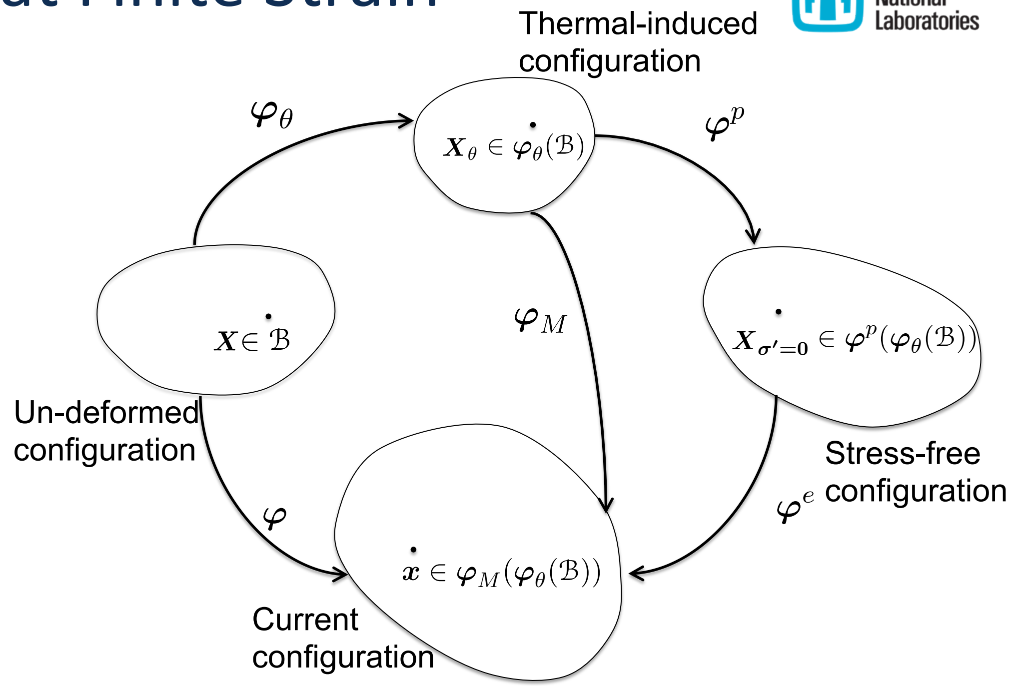

Multiplicative decomposition of the thermo-hydro-mechanics problem

---

Multiplicative decomposition of skeleton deformation gradient

$$\boldsymbol{F} = \frac{\partial \boldsymbol{\varphi}(\boldsymbol{X}, t)}{\partial \boldsymbol{X}} = \boldsymbol{F}_M \cdot \boldsymbol{F}_\theta \;\; ; \;\; \boldsymbol{F}_\theta = \frac{\partial \boldsymbol{\varphi}_\theta(\boldsymbol{X}, t)}{\partial \boldsymbol{X}} \;\; ; \boldsymbol{F}_M = \frac{\partial \boldsymbol{\varphi}_M(\boldsymbol{X}_\theta, t)}{\partial \boldsymbol{X}_\theta}$$

Concept of Effective Stress

$$\boldsymbol{\sigma} = \boldsymbol{\sigma'} - Bp^{\mathrm{f}}\boldsymbol{I}, \qquad \boldsymbol{P}(\boldsymbol{F}, \boldsymbol{z}, p^f, \theta) = \boldsymbol{P'}(\boldsymbol{F}, \boldsymbol{z}, \theta) - JBp^f \boldsymbol{F}^{-T}$$

$$B = 1 - \frac{K}{K_{\mathrm{s}}} \qquad \boldsymbol{P}(\boldsymbol{F}_M, \boldsymbol{z}, p^f) = \boldsymbol{P'}(\boldsymbol{F}_M, \boldsymbol{z}) - JBp^f \boldsymbol{F}^{-T},$$

Strong Form of THM Problem at Finite Strain

❑ Balance of Linear Momentum

$$\boxed{\nabla^{\boldsymbol{X}} \cdot \boldsymbol{P} + J(\rho^s + \rho^f)\boldsymbol{G} = \boldsymbol{0}}$$

where $$\boldsymbol{P}(\boldsymbol{F}_M, \boldsymbol{z}, p^f) = \boldsymbol{P}'(\boldsymbol{F}_M, \boldsymbol{z}) - JBp^f \boldsymbol{F}^{-T},$$

Total Stress

Effective Stress

❑ Balance of Mass

$$\boxed{\left(\frac{B}{J} - 3\alpha_{\mathrm{s}}(\theta - \theta_o)\right)\dot{J} + \frac{1}{M}\dot{p}^{\mathrm{f}} - 3\alpha^{\mathrm{m}}\dot{\theta} + \frac{1}{\rho_f}\nabla^{\boldsymbol{X}} \cdot \boldsymbol{W} = 0.}$$

where

$$\boldsymbol{W} = J\boldsymbol{F}^{-1} \cdot \boldsymbol{w}.$$ and $$\boldsymbol{w} = \rho_{\mathrm{f}}\boldsymbol{k} \cdot \left[-\nabla^{\boldsymbol{x}} p^{\mathrm{f}} + \rho_{\mathrm{f}}(\boldsymbol{G} - \boldsymbol{a}^{\mathrm{f}})\right] - \rho_{\mathrm{f}} s_T \nabla^{\boldsymbol{x}} \theta,$$

Darcian flow

Soret effect (neglected here)

❑ Thermal energy transport equation

$$\boxed{c_{\boldsymbol{F}}\dot{\theta} = [D_{\mathrm{mech}} - H_\theta] + [-\nabla^{\boldsymbol{X}} \cdot \boldsymbol{Q}_\theta - \frac{\Phi^{\mathrm{f}} c_{\boldsymbol{F}\mathrm{f}}}{\rho_{\mathrm{f}}}\boldsymbol{W} \cdot \boldsymbol{F}^{-T}\nabla^{\boldsymbol{X}}\theta + R_\theta],}$$

where

$$H_\theta = H_\theta^{\mathrm{s}} + H_\theta^{\mathrm{f}},$$

Total Structural Heating

and $$H_\theta^{\mathrm{s}} = -\theta\frac{\partial}{\partial\theta}\boldsymbol{P}' : \dot{\boldsymbol{F}} = -3K\alpha_{sk}\theta\frac{\dot{J}}{J}$$ Solid Structural Heating

$$H_\theta^{\mathrm{f}} = -\theta\frac{\partial}{\partial\theta}3\alpha^{\mathrm{m}}(\theta - \theta_o)\dot{p}^{\mathrm{f}} = -3\alpha^{\mathrm{m}}\theta\dot{p}^{\mathrm{f}}.$$ Fluid contribution

Remarks on Estimating Effective Thermal Conductivity from Microstructures

- Volume averaging effective conductivity

$$\boldsymbol{k}_\theta = \phi^{\mathrm{f}} \boldsymbol{k}_\theta^{\mathrm{f}} + (1 - \phi^{\mathrm{f}}) \boldsymbol{k}_\theta^{\mathrm{s}}$$

(cf. Preisig & Prevost, IJGGC 2011)

- Homogenized effective conductivity via Eshelby equivalent inclusion method (for spherical inclusions)

$$\boldsymbol{k}_\theta = \left(k_\theta^{f} + \frac{\phi^{\mathrm{f}} (k_\theta^{\mathrm{s}} - k_\theta^{\mathrm{f}}) k_\theta^{\mathrm{f}}}{(k_\theta^{\mathrm{s}} - k_\theta^{\mathrm{f}}) \phi^{\mathrm{f}} + k_\theta^{\mathrm{f}}} \right) \boldsymbol{I}$$

(cf. Zhou & Meschke, IJNAMG 2013)

Important Note: In general, the temperature of the pore-fluid and solid skeleton are not the same in the same REV, unless sufficient diffusion takes place. This difference is neglected in current formulation.

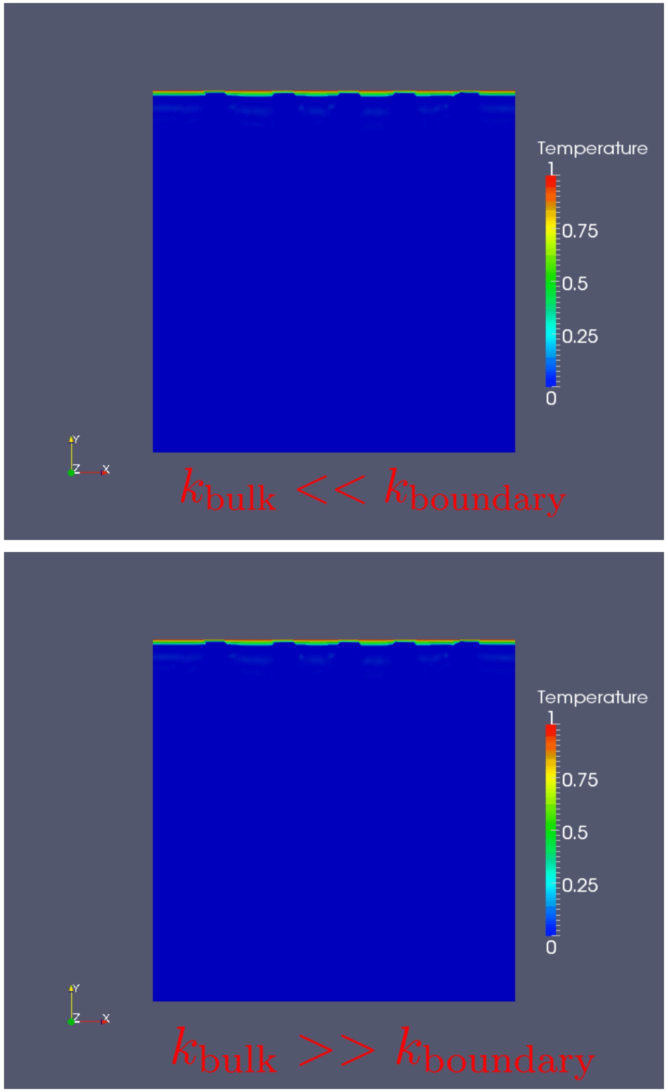

Solution of transient heat equation of two-phase materials

Stabilization for Equal-order THM Finite Element

❑ Combined Inf-sup Condition (not satisfied)

$$\sup_{\boldsymbol{w}^h \in V_{\boldsymbol{u}}{}^h} \frac{\int_{\mathcal{B}} \left(p^{\mathrm{f}h} B + 3\theta K \alpha_{\mathrm{sk}} \right) \nabla^{\boldsymbol{x}} \cdot \boldsymbol{w}^h \; d\mathrm{V}}{||\boldsymbol{w}^h||_{\boldsymbol{V}_{\boldsymbol{u}}^{\boldsymbol{h}}}} \geq C_o \left(||p^{\mathrm{f}h}||_{V_p^h} + ||\theta^h||_{V_\theta^h} \right)$$

❑ Combined Weak Inf-sup Condition (still satisfied)

$$\sup_{\boldsymbol{v}^h \in \boldsymbol{V}_{\boldsymbol{u}}^{\boldsymbol{h}}, \boldsymbol{v} \neq \boldsymbol{0}} \frac{\int_{\mathcal{B}} \left(p^{\mathrm{f}h} B + 3K \alpha_{\mathrm{sk}} \theta^h \right) \nabla^{\boldsymbol{x}} \cdot \boldsymbol{v}^h \; d\mathrm{V}}{||\boldsymbol{v}^h||_1} \geq C_1 \left(||p^{\mathrm{f}h}||_{V_{p^{\mathrm{f}}}^h} + ||\theta^h||_{V_\theta^h} \right) - C_2 h \left(|| \nabla^{\boldsymbol{x}} p^{\mathrm{f}h} ||_{V_{p^{\mathrm{f}}}^h} + || \nabla^{\boldsymbol{x}} \theta^h ||_{V_\theta^h} \right)$$

❑ Projection-based Stabilization

$$\hat{H}^{\mathrm{stab}}(\psi, p_{n+1}^{\mathrm{f}h}, \theta_{n+1}^h) = \sum_{K \in \mathcal{B}} \int_K C(\psi - \mathit{\Pi}\psi) B \left(p_{n+1}^{\mathrm{f}h} - p_n^{\mathrm{f}h} - \mathit{\Pi}(p_{n+1}^{\mathrm{f}h} - p_n^{\mathrm{f}h}) \right) d\mathrm{V}$$
$$+ \sum_{K \in \mathcal{B}} \int_K C(\psi - \mathit{\Pi}\psi)(3\alpha^m) \left(\theta_{n+1}^h - \theta_n^h - \mathit{\Pi}(\theta_{n+1}^h - \theta_n^h) \right) d\mathrm{V} \; .$$

Stabilization parameter

Interpolated temperature changes

Projected element-wise constant temperature changes

No stabilization

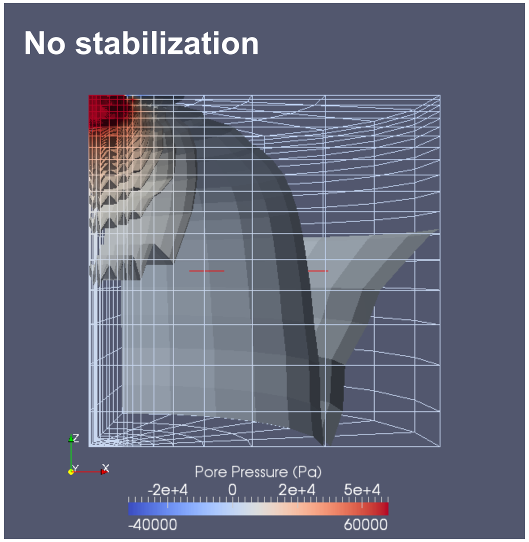

With stabilization

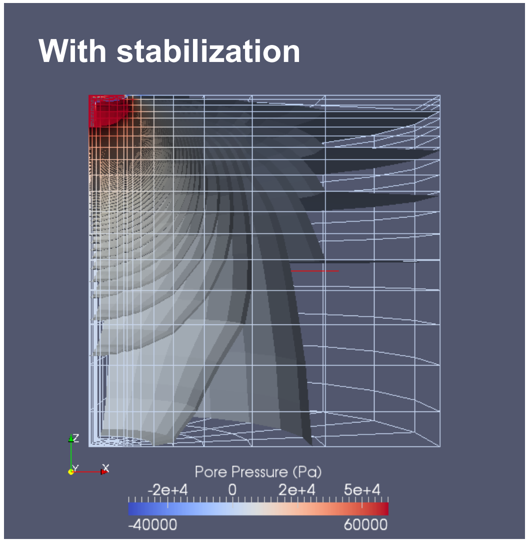

Combined F-bar Formulation

- Isochoric-volumetric split (Hughes 1975, Simo 1975)

$$\boldsymbol{F} = \boldsymbol{F}_{\mathrm{vol}} \cdot \boldsymbol{F}_{\mathrm{iso}}$$

- Replacing volumetric split with assumed term

$$\overline{\boldsymbol{F}} = \underset{\substack{\uparrow \\ \text{Modified det(F)}}}{\bar{J}^{1/3}} \boldsymbol{F}_{\mathrm{iso}} = \bar{J}^{1/3} \underset{\substack{\uparrow \\ \text{Original det(F)}}}{J^{-1/3}} \boldsymbol{F}$$

Relaxing too much, we get instability
Relaxing too little, we get the volumetric locking

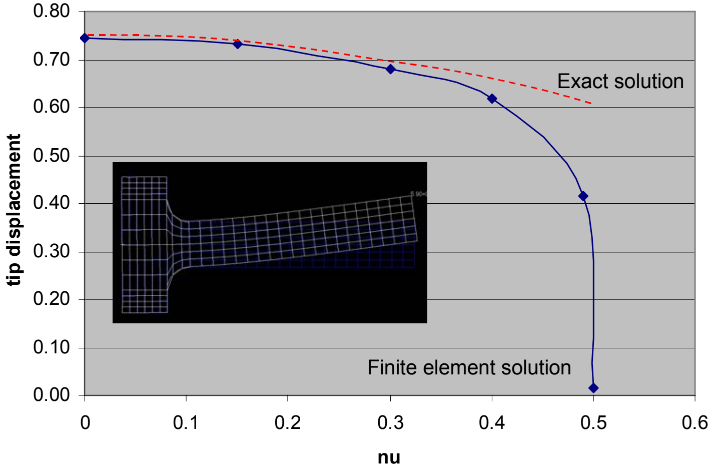

Standard F leads to Volumetric Locking

- Combined F-bar approach

$$\widetilde{\boldsymbol{F}} = \alpha \boldsymbol{F} + (1 - \alpha) \overline{\boldsymbol{F}}.$$

← Why this is wrong?

- Current Approach via Lie algebra

$$\widetilde{J} = \exp\Big(\frac{1-\beta}{\mathrm{V}_{\mathcal{B}^e}} \int_{\mathcal{B}^e} \log J \; \mathrm{dV} + \beta \log J\Big).$$

$$\widetilde{J}_M = \exp\Big(\log \widetilde{J} - 3\big(\frac{1-\beta}{\mathrm{V}_{\mathcal{B}^e}} \int_{\mathcal{B}^e} \alpha_{sk}(\theta - \theta_o) \; \mathrm{dV} + \beta\alpha_{sk}(\theta - \theta_o\,)\big)\Big)$$

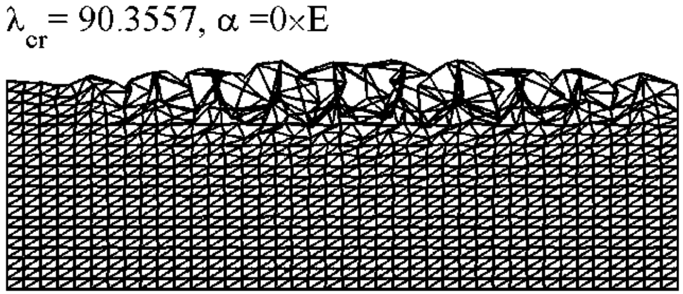

Pure F-bar leads to instability (Brocardo, Micheloni, Krysl, IJNME2009)

See Sun, Ostien, Salinger, International Journal for Numerical and Analytical Methods in Geomechanics, 2013

Optimal Stabilization Parameter Estimation

1D poromechanics governing equation

$$c\frac{\partial^2 \hat{p}}{\partial x^2} = \frac{\partial \hat{p}}{\partial t}, \qquad c = \frac{k}{\mu}\frac{M'H}{H + \nu\beta M'}; M' = \frac{M(K+4G/3)}{K+4G/3+B^2M}$$

Three node stencil (standard Galerkin method)

$$-\hat{p}_{A-1} + 2\hat{p}_A - \hat{p}_{A-1} + \frac{h^2}{6\vartheta c\Delta t}(\hat{p}_{A-1} + 4\hat{p}_A + \hat{p}_{A+1}) = 0$$

Three node stencil (Stabilized Galerkin method)

$$-\hat{p}_{A-1} + 2\hat{p}_A - \hat{p}_{A-1} + \frac{h^2}{12\vartheta c\Delta t}[(2-\gamma)\hat{p}_{A-1} + (8+2\gamma)\hat{p}_A + (2-\gamma)\hat{p}_{A+1}] = 0$$

Growth/decay rate

$$\cosh\frac{h}{(\sqrt{\vartheta c\Delta t})^h} = \frac{(1+h^2/\vartheta c\Delta t)(4+\gamma)/6}{(1-h^2/\vartheta c\Delta t)(2-\gamma)/12}$$

To have real growth/decay rate, we need

$$\gamma > 2 - 12\frac{\vartheta c\Delta t}{h^2} > 0 \qquad \boxed{\gamma = (2 - 6\frac{\vartheta c\Delta t}{h^2})\left(\frac{1}{2} + \frac{1}{2}\tanh(2 - 12\frac{\vartheta c\Delta t}{h^2})\right)}$$

Safety factor

Turn off stabilization without introducing switch

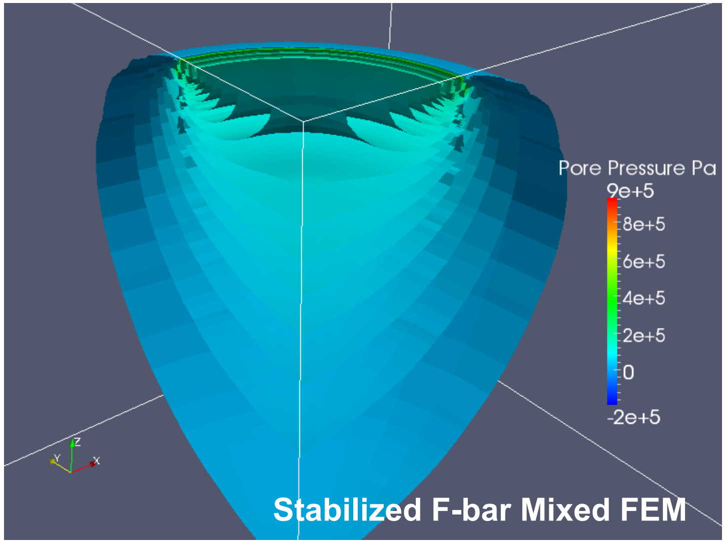

Stabilized F-bar Mixed FEM

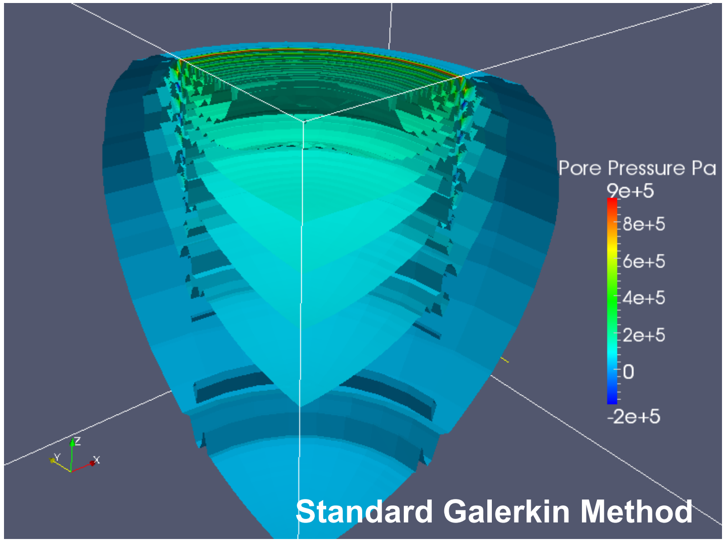

Standard Galerkin Method

See Sun, Ostien, Salinger, International Journal for Numerical and Analytical Methods in Geomechanics, 2013

Thermo-hydro-mechanical Responses of Porous Sphere in Thermal Reservoir

X Under-diffusion with spurious patterns

✓ Diffusion with optimal stabilization

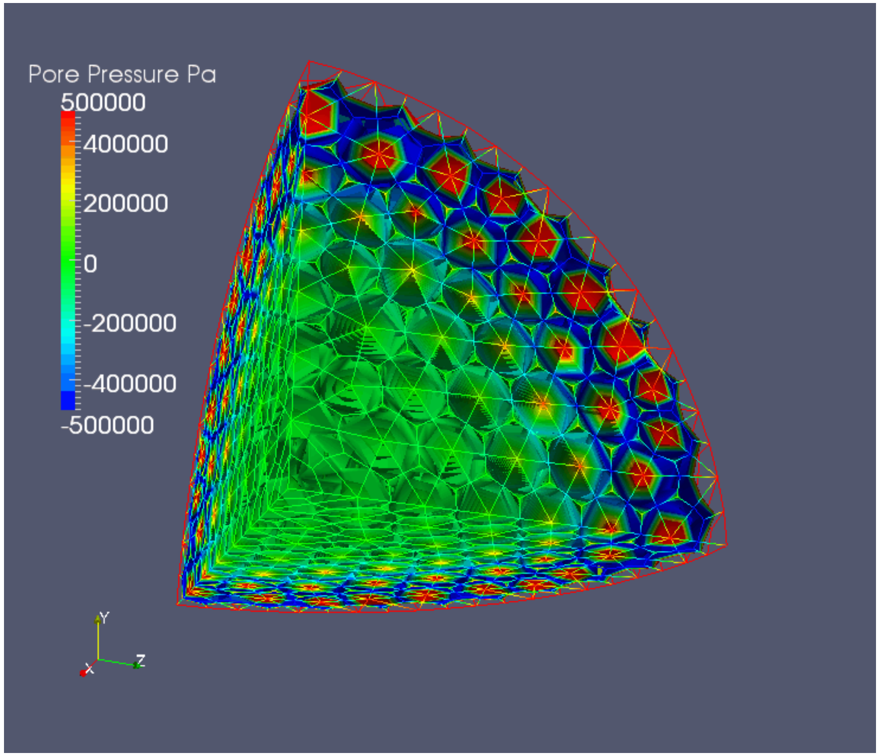

without Stabilization

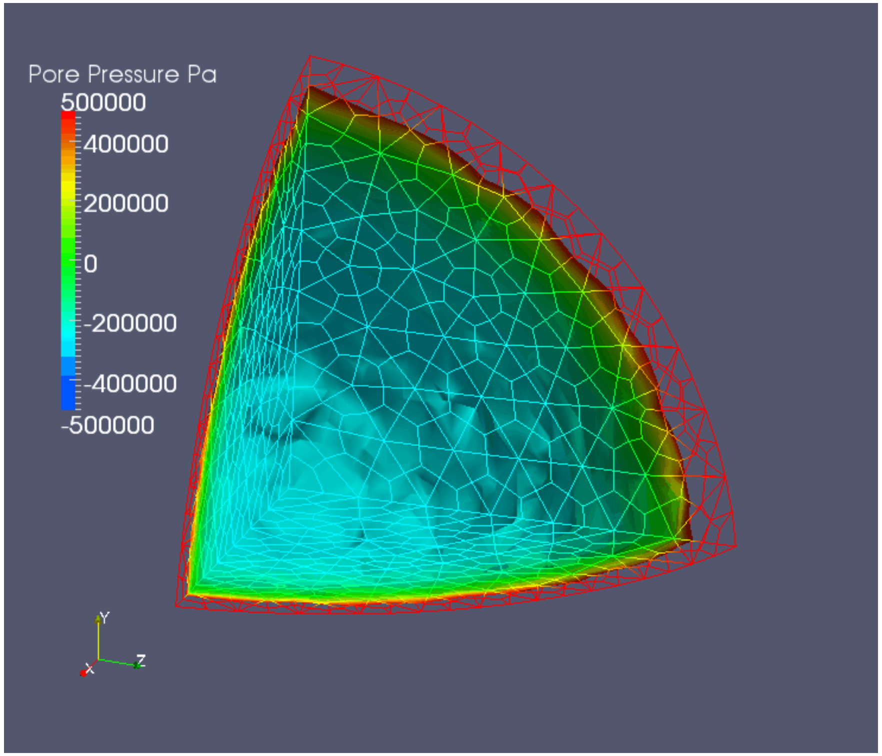

with Stabilization

Thermo-hydro-mechanical Responses of Porous Sphere in Thermal Reservoir

X Under-diffusion with spurious patterns ✓ Diffusion with optimal stabilization

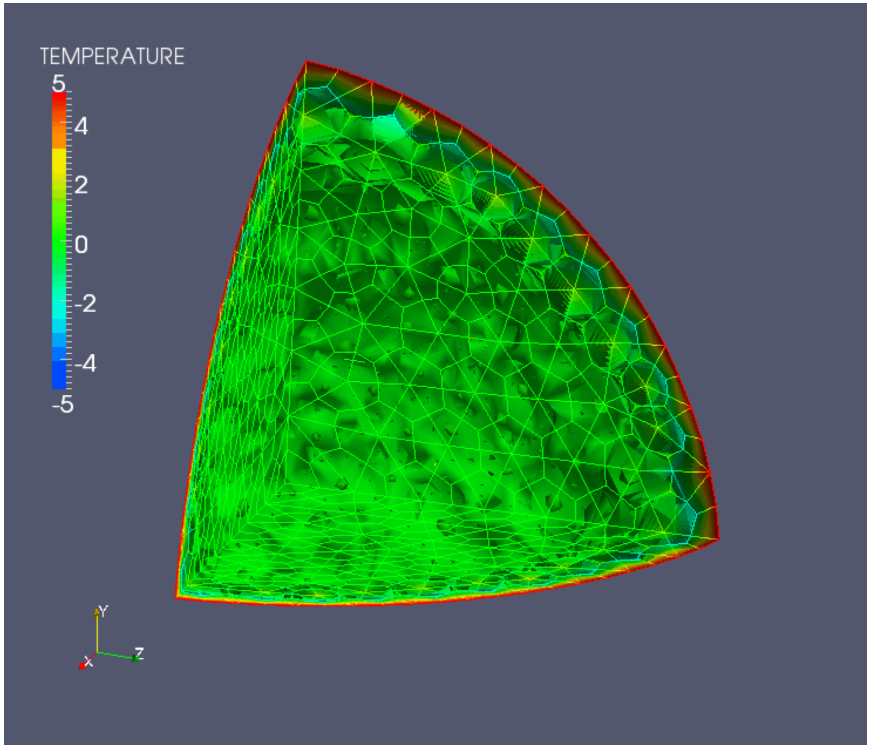

without Stabilization

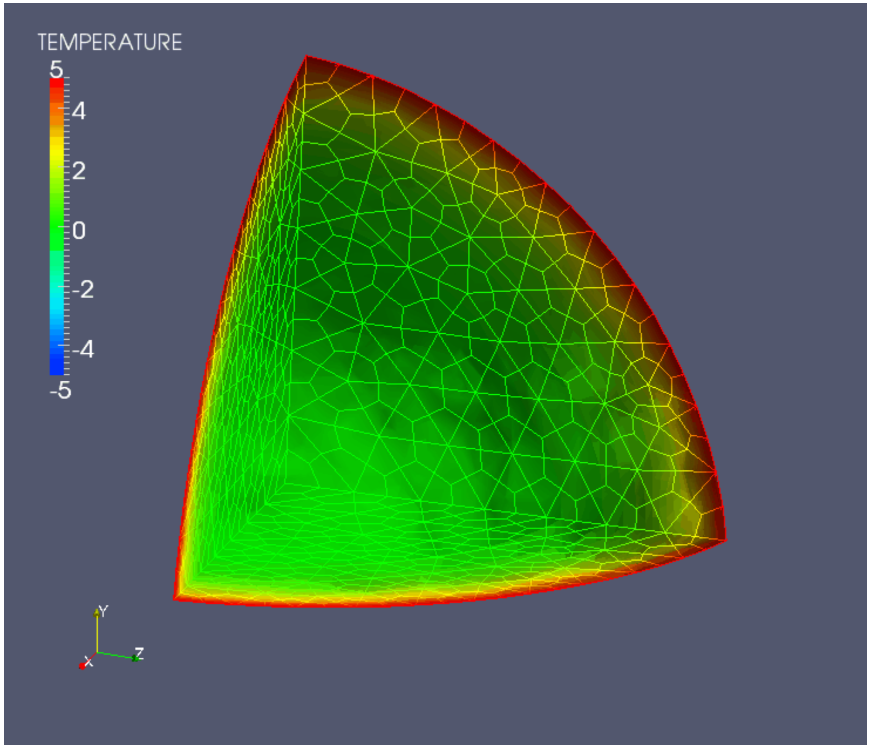

with Stabilization

Generalized Mandel-Cryer Effect for THM problems

✓ Solution with optimal stabilization (Stabilization parameter C=2)

X Over-diffusion solution (Stabilization parameter C=200000)

Temperature

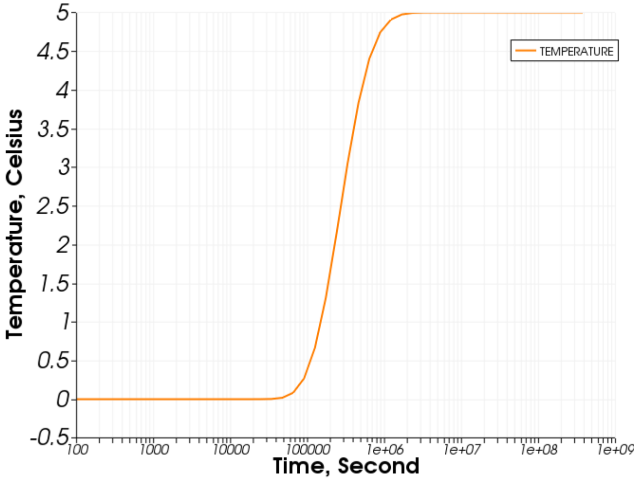

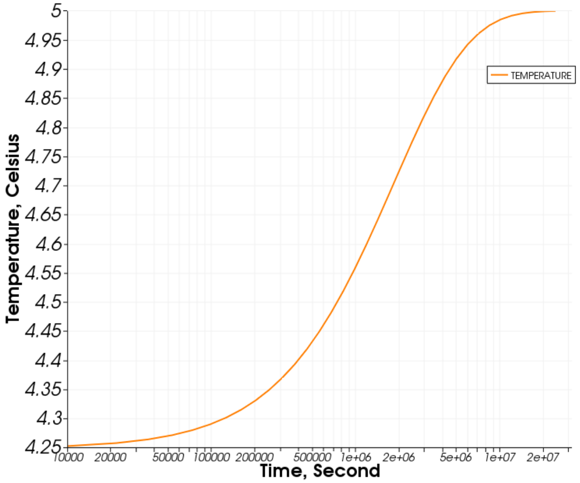

Pore pressure

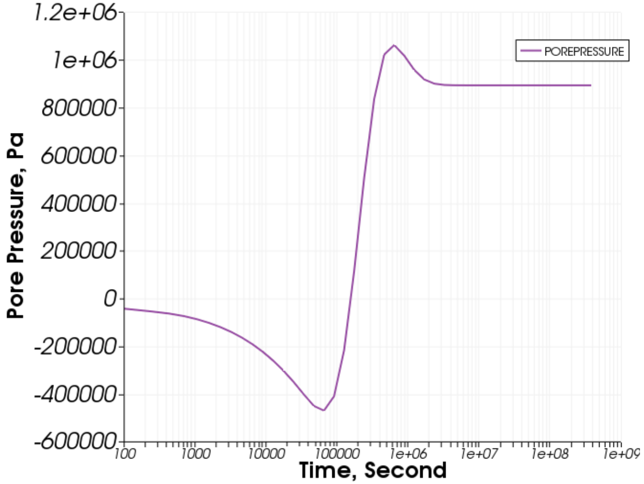

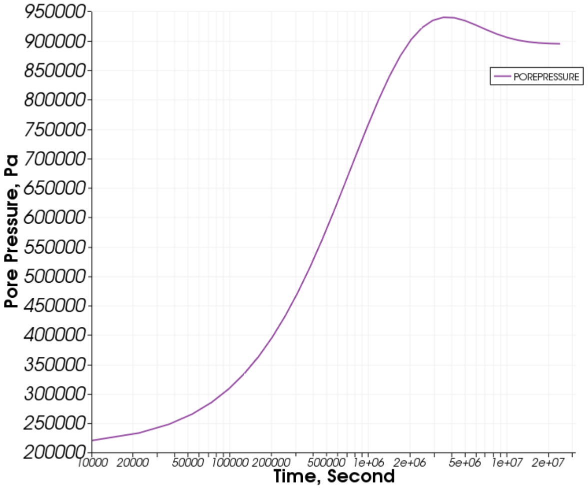

Heat pump problem

1. Hot liquid is injected into a elasto-plastic porous medium
2. Pore-fluid diffusion and heat diffusion occur at different rate
3. Porous medium expands even though no mechanical load is applied.

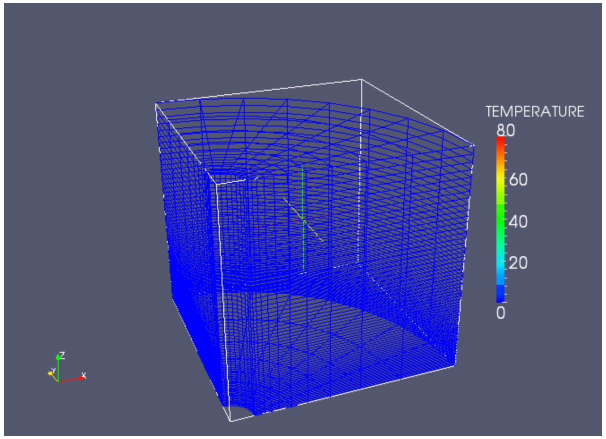

Temperature

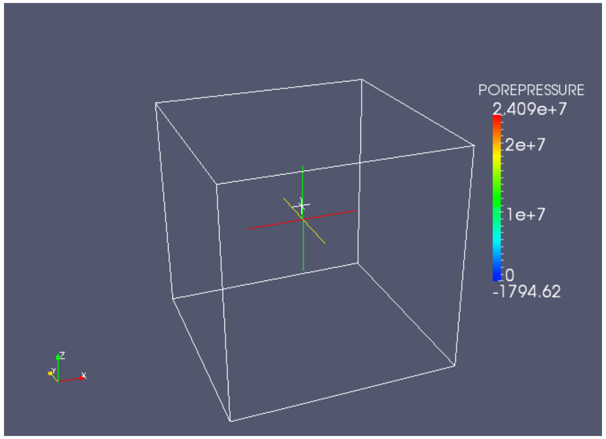

Pore pressure

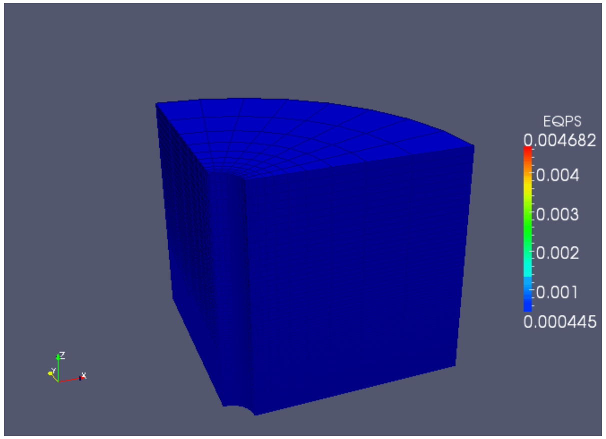

equivalent plastic strain

Conclusion and Future Perspective

- For the 1st time, A fully coupled, finite deformation, stabilized thermo-hydro-mechanics finite element model is implemented.
- This model preserves Mandel-Cryer effect, and is able to eliminate spurious oscillation due to the lack of inf-sup condition.
- Localization element is introduced as localization limiter to cure mesh dependence.
- Unsaturated flow will be further tested against analytical solutions and classical problems in the literatures.
- Further validation and verification tests must be performed to ensure correctness of the proposed model .
- In some cases the tangential matrix might be ill-conditioned (high condition number). As a result, pre-conditioner is needed.

Bibliography

- W.C. Sun, J.T. Ostien and A.G. Salinger, a stabilized enhanced deformation gradient finite element formulation for strongly coupled poromechanical simulations at finite strain, in press, International Journal for Numerical and Analytical Methods in Geomechanics.
- J.W. Foulk III, W.C. Sun, G. Wagner, C. San Marchi, B. Somerday, the evolution of hydrogen concentration in 21 Cr-6Ni-9Mn austenitic stainless steel, in preparation.
- A. Mota, W.C. Sun, J.T. Ostien, J.W. Foulk III and K.N., Long, Lie-group interpolation and variational recovery for internal variables, in press, *Computational Mechanics*.
- W.C. Sun, Y.L. Young, Influence of soil heterogeneity on finite strain sedimentation-consolidation phenomena, submitted to *International Journal for Numerical and Analytical Methods in Geomechanics*.
- W.C. Sun, M.R. Kuhn, J.W. Rudnicki, Permeability in shear bands: a multiscale DEM-LBM analysis on shear band, in press, An unified method to predict diffuse and localized instabilities in sands, accepted, *Geomechanics and Geoengineering*.
- W.C. Sun, J.W. Rudnicki, J.E. Andrade and P. Eichhubl, Connecting microstructural attributes and permeability from 3-D tomographic images of in situ compaction bands using multi-scale computation, *Geophysical Research Letter*, doi : 10.1029/2011GL047683, 2011.
- W.C Sun, J.E. Andrade, J.W. Rudnicki, A multiscale method for characterization of porous microstructures and their impact on macroscopic effective permeability*, International Journal of Numerical Methods in Engineering*, Vol. 88, No.12, 1260-1279, 2011.
- R.I. Borja and W.C. Sun, Co-seismic sediment deformation during the 1989 Loma Prieta Earthquake, *Journal of Geophysical Research*, Vol.113, B08314,doi:10.1029/2007JB005265, 2008.
- R.I. Borja and W.C. Sun, Estimating inelastic sediment deformation from local site response simulations, *Acta Geotechnica*, Vol. 2, Number 3, 2007, pp.183-195.

Thank you!

Extra Slides

Formulation of the localization element

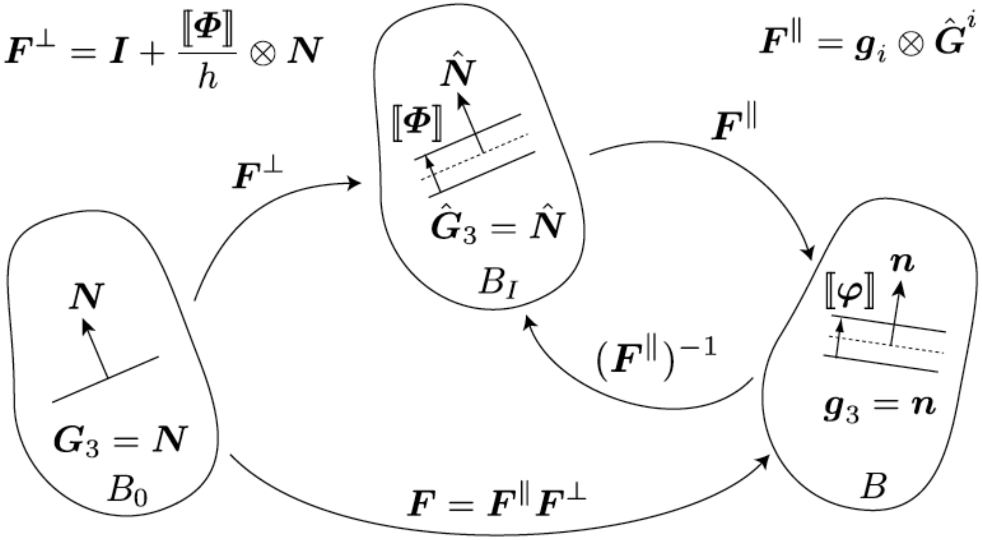

$$\hat{G}_A \parallel G_A \longrightarrow F = F^{\|} + \frac{\llbracket \varphi \rrbracket}{h} \otimes N$$

$$\llbracket \Phi \rrbracket = (F^{\|})^{-1} \llbracket \varphi \rrbracket$$

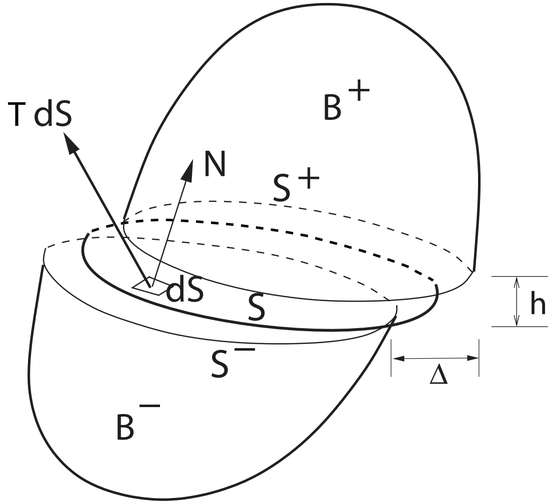

From Yang, Mota Ortiz, 2006; Foulk et al 2013

Deformation power of the solid skeleton

$$
\begin{aligned}
P^D &= \sum_{\pm} \int_{B_0^{\pm}} P \cdot \dot{F} \, dV + \int_{S_0} P \cdot \dot{F} h \, dS \\
&= \sum_{\pm} \int_{B_0^{\pm}} P \cdot \dot{F} \, dV + \int_{S_0} P \cdot \left[\dot{F}^{\|} h + \llbracket \dot{\varphi} \rrbracket \otimes N \right] dS \\
&= \sum_{\pm} \int_{B_0^{\pm}} P \cdot \dot{F} \, dV + \int_{S_0} \left[h P \cdot \dot{F}^{\|} + T \cdot \llbracket \dot{\varphi} \rrbracket \right] dS
\end{aligned}
$$

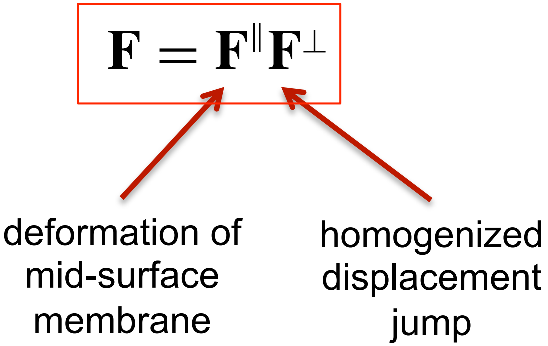

$$\boxed{\mathbf{F} = \mathbf{F}^{\|} \mathbf{F}^{\perp}}$$

deformation of mid-surface membrane

homogenized displacement jump

Globally undrained Simple Shear Test of Fully saturated media with flow barrier in the surface element (Pore Pressure)

Without sealed rock joint

With sealed rock joint

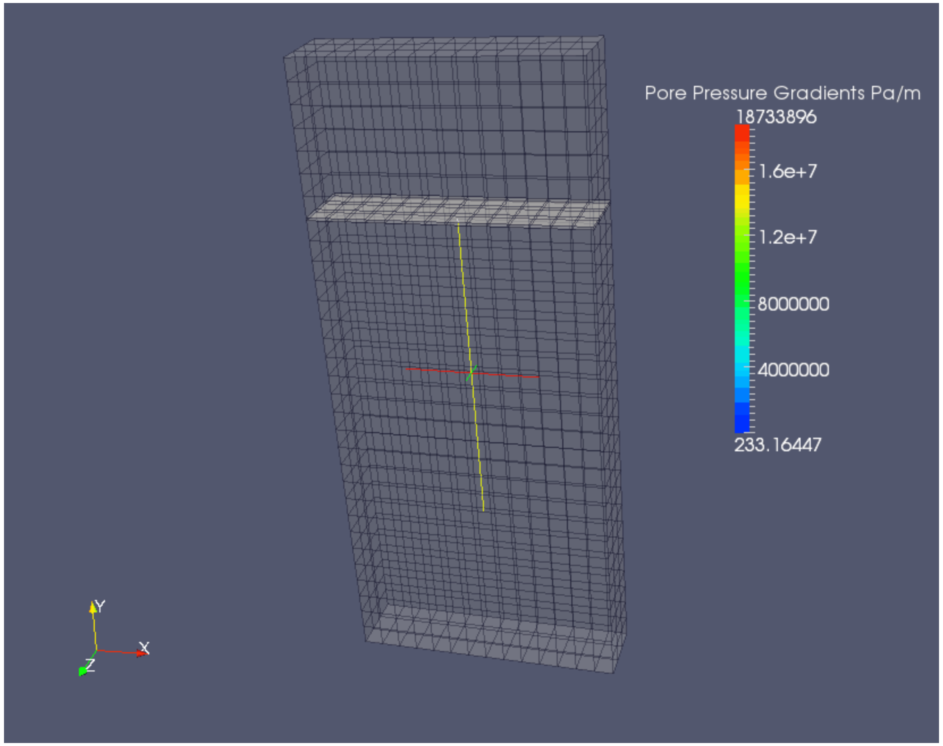

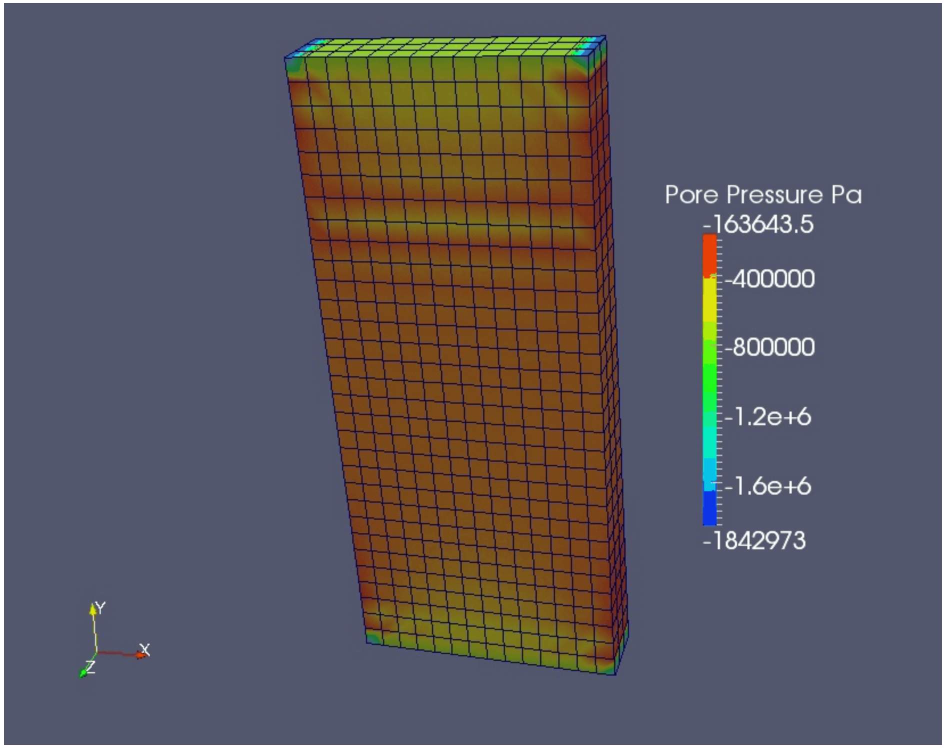

- In geometrical nonlinear regime, pore-fluid flow is significantly influenced by geometrical changes.
- Capturing localized hydraulic features triggered by deformation is important to analyze overall reservoir properties.